LIMNOLOGY
and
OCEANOGRAPHY: METHODS

Limnol. Oceanogr.: Methods 8, 2010, 592–609

Estimating methane emissions from northern lakes using ice-bubble surveys

Katey M. Walter Anthony[2], Dragos. A. Vas[2], Laura Brosius[2], F. Stuart Chapin III[1], Sergey A. Zimov[3], and Qianlai Zhuang[4]*

[1]Institute of Arctic Biology, Irving Building I, University of Alaska Fairbanks, Fairbanks, AK 99775-7000
[2]Water and Environmental Research Center, University of Alaska Fairbanks, Fairbanks, AK 99775-7000
[3]Northeast Science Station, P.0. Box 18, Cherskii, Republic of Sakha (Yakutia), Russia
[4]College of Science, Department of Earth and Atmospheric Sciences, Purdue University, West Lafayette, IN 47907

Abstract

The magnitude and variability in methane (CH_4) emissions from lakes are uncertain due to limitations in methods for quantifying the patchiness of ebullition (bubbling). We present a field method to estimate an important and highly uncertain source: ebullition from northern lakes. We defined four classes of CH_4 bubble clusters trapped in lake ice representing distinct types of biogenic ebullition seeps that differed in flux rate. Mean annual ebullition determined through long-term (up to 700 d) continuous flux measurements of 31 seeps in three Siberian and one Alaskan lake was (mean ± standard error, 4-10 seeps per class; g CH_4 $seep^{-1}$ y^{-1}): A, 6 ± 4; B, 48 ± 11; C, 354 ± 52; Hotspot, 1167 ± 177. Discrete-seep ebullition comprised up to 87% of total emissions from Siberian lakes when diffusive flux and background and seep ebullition were considered together. Including seep ebullition increased previous estimates of lake CH_4 emissions based on traditional methods 5- to 8-fold for Siberian and Alaskan lakes. Linking new ebullition estimates to an established biogeochemical model, the Terrestrial Ecosystem Model, increased previous estimates of regional terrestrial CH_4 emissions 3- to 7-fold in Siberia. Assessment of the method revealed that ebullition seeps are an important component of the terrestrial CH_4 budget. They are identifiable by seep type by independent observers; they are consistent predictors of flux rate in both Siberia and Alaska; and they allow quantification of what was previously a large source of uncertainty in upscaling CH_4 emissions from lakes to regions.

In his Russian Christmas story, A. N. Tolstoy wrote about children ice-skating on frozen lakes and pausing to light methane (CH_4) bubbles trapped in lake ice to heat their tea. Although Russian children have been reading about these bubbles in ice for more than a century, recognition of their importance as an atmospheric CH_4 source is only now being made in the scientific literature. CH_4 is a potent greenhouse gas with ~25 times the radiative effect of carbon dioxide (CO_2) on a 100-y time scale (Boucher et al. 2009). Although CH_4 production was one of the earliest microbiological processes to be studied, natural sources of atmospheric CH_4 are still not well understood. The largest natural source of atmospheric CH_4, global wetlands, has an uncertainty of 95% (92-260 Tg CH_4 y^{-1}; Walter et al. 2001; Chen and Prinn 2006) and typically does not include emissions from lakes (Matthews and Fung 1987; Matthews 2000; others). Unlike wetlands, most lake sediments remain unfrozen year-round, producing and emitting CH_4. This article presents a new technique to quantify a potentially large source of atmospheric CH_4, bubbling from arctic and sub-arctic lakes, that has not been incorporated in previous regional or global CH_4 budgets (Cicerone and Oremland 1988; Zhuang et al. 2004; IPCC 2007).

*Corresponding author: (*formerly published as Katey M. Walter*) Current address: Water and Environmental Research Center, University of Alaska Fairbanks, Fairbanks, AK 99775-7000

Acknowledgments

We thank S. P. Davidov for active contributions throughout the research; D. A. Draluk and A. Strohm for assistance with long-term flux measurements in winter; P. M. Anthony, C. Arp, M. L. Geai, L. McFadden, L. Oxtoby, E. T. Ricter, A. Strohm, and C. Thompson for additional field and lab assistance; J. Chanton for use of his stable isotope laboratory; the Northeast Science Station in Cherskii, Russia and Toolik Field Station, Alaska for logistic support; and M. Engram, D. Valentine, B. Finney, and R. Ruess for editorial comments on the manuscript. Siberian research funding was provided by the National Science Foundation through the Russian-American Initiative on Shelf-Land Environments of the Arctic (RAISE) of the Arctic System Science Program (ARCSS) and Polar Programs grant #0093677, Environmental Protection Agency STAR Fellowship Program, and the NASA Headquarters under the Earth System Science Fellowship Grant NGT5. The Alaskan research was funded by NSF Polar Programs IPY grant #0732735 and DOE #DE-NT0005665.

DOI 10:4319/lom.2010.8.592

Lakes are a prominent landscape feature in the North occupying up to 30% of land surface area (Zimov et al. 1997; Semiletov 1999; Riordan et al. 2006). Arctic and boreal lakes are also known to be net emitters of CH_4 (Kling et al. 1992; Zimov et al. 1997; Semiletov 1999; Walter et al. 2006). Methane emission from lakes can occur by three pathways: transport through gas-conducting tissues of emergent plants (Chanton et al. 1989; Chanton 2005), molecular diffusion, and ebullition (bubbling). Emergent plants, where present, are important conduits in shallow, productive lakes (Juutinen et al. 2003), but many arctic and sub-arctic lakes are open water bodies where CH_4 emission occurs primarily by molecular diffusion (Kling et al. 1992) and ebullition (Zimov et al. 1997, 2001; Walter et al. 2006) (Table 1). Ebullition is a particularly effective mode of emission because it transports CH_4 directly from sediments to the atmosphere, largely bypassing oxidation that can occur in the water column or in the oxygenated soils adjacent to plant roots (Chanton 2005).

Methane, formed during anaerobic decomposition of plant and animal remains in lake bottoms, is only sparingly soluble in water, so CH_4 produced in sediments quickly reaches saturation and comes out of solution as bubbles. Bubbles are released sporadically in response to change in bottom currents (Joyce and Jewell 2003), decrease in hydrostatic pressure caused by a reduction in water level (Bartlett et al. 1988), decline in atmospheric pressure, or if bubble buoyancy exceeds threshold (Mattson and Likens 1990; Casper et al. 2000; Glaser et al. 2004; Tokida et al. 2007).

Table 1 summarizes the methods and CH_4 emission rates reported from lakes globally in the scientific literature. Many lake-CH_4 emission studies were based on estimates of diffusive flux, which can be calculated using a boundary-layer model and measurements of wind speed and dissolved CH_4 concentration in the surface water (Kling et al. 1992; Juutinen et al. 2009). Ebullition is also a well-known phenomenon (Keller and Stallard 1994; Casper et al. 2000; others), and some studies suggested that accounting for ebullition could make lakes an important component of the global atmospheric methane budget: 8-55 Tg CH_4 y^{-1} (Smith and Lewis 1992; Bastviken et al. 2004; Walter et al. 2007), which is up to 10% of all natural and anthropogenic sources. Ebullition is challenging to measure because bubbles occur sporadically and haphazardly across the surface of lakes. This makes sampling particularly difficult as seemingly minor misses during collection give large errors in the resulting estimate. Such errors also make it difficult to detect statistically significant differences among treatments or ecosystems. Bubble fluxes have been measured with floating chambers or submerged bubble traps, both of which are often deployed in designs that stratify sampling within lakes by littoral versus pelagic, sandy sediment versus organic sediment, etc., to account for between-lake-zone ebullition patterns (Keller and Stallard 1994; Huttunen et al. 2003; Bastviken et al. 2004). Within these zones, scientists placed traps randomly rather than over discrete ebullition seeps. Most measurements of ebullition were short-term (minutes to days). Long-term continuous measurements are rare, and even the most innovative techniques using automated bubble traps did not quantify the patchiness of bubbling by measuring discrete ebullition seeps (Varadharajan 2009).

Here we present a new technique that uses the spatial patchiness of ebullition as a basis for stratifying measurements, thereby providing a rigorous platform for scaling CH_4 fluxes to entire lakes and regions. The "ice-bubble ebullition classification method" takes advantage of ice formation on lakes to identify and map the distribution of discrete, fixed points of bubbling (ebullition seeps) that are recognized based on distinct patterns of ebullition bubbles trapped in lake ice. Walter et al. (2006) used this method to demonstrate the importance of CH_4 release associated with thawing permafrost in Siberia as a positive feedback to climate warming. The method is presented here in detail using updated ebullition values for four distinct seep classes based on the combination of long-term flux measurements made on discrete seeps in three Siberian lakes in 2003-2004 and on the same classes of seeps in an Alaskan lake during 2008-2010.

This article has four goals: to (1) describe the new method of quantifying discrete ebullition seep emissions in lakes; (2) assess uncertainties associated with the method, including variability among seep classes, observers, and variability within and among lakes; (3) apply the method at nine lakes in Alaska and Siberia to compare new emission estimates to previous studies of the same lakes using traditional methods; and (4) demonstrate the importance of this method for including lake-ebullition seeps in bottom-up biogeochemical modeling of terrestrial ecosystem sources of atmospheric CH_4 at high latitudes.

Materials and procedures

Study sites—We collected gas samples from biogenic seeps during 2003-2010 on lakes in the continuous permafrost zone in the Kolyma Lowland region in northeast Siberia near the Northeast Science Station in Cherskii (68.7°N, 161.3°E), the North Slope of Alaska's Brooks Range near Toolik Lake Field Station (68.6°N, 149.5°W), the northern Seward Peninsula (65.5°N, 164.4°W), and from lakes in the discontinuous permafrost zone of interior Alaska near Fairbanks (64.9°N, 147.8°W). We conducted long-term CH_4 flux measurements in three Siberian thermokarst lakes (Shuchi L., Tube Dispenser L., and Grass L.) from 7 May 2003-1 Jun 2004 and in one thermokarst lake (Goldstream L.) in interior Alaska, near Fairbanks (64.9°N, 147.8°W) from 17 Jun 2008-18 May 2010. Shuchi L., Tube Dispenser L. and Goldstream L., with maximum water depths of 11 m, 17 m, and 2.2 m, respectively, all had active thermokarst (permafrost thaw) along some margins. Grass L., a smaller lake with a thick wetland moat, had no apparent thermokarst and was 12 m deep. All lakes exhibited thermal stratification in summer.

Gas composition and stable isotope measurements—To determine variability in CH_4 concentration by seep type and

Table 1. Summary of published methane emissions from tropical, temperate, and arctic lakes by diffusion (D) and ebullition (E). Minimum, maximum, and seasonal averages for measurements of methane flux are given in mg CH_4 m^{-2} d^{-1}. Methane concentrations (% CH_4) were measured in bubble samples.

Zone/ Reference	Object	Mode	Method†	% CH_4	Min	Max	Seasonal average
Tropics							
Keller and Stallard 1994	Tropical man-made lake	D	C				12.4
Keller and Stallard 1994	Tropical man-made lake	E	BT,C	67% to 77%	10	2000	47-1302
Bartlett et al. 1988	Amazon floodplain	D	C				8.3
Bartlett et al. 1988	Amazon floodplain	E	C	58% to 72%	0	2997	17-346
Temperate							
Miller and Oremland 1988	Searsville L. (freshwater reservoir), CA	D + E	C				160
Miller and Oremland 1988	Searsville L. (freshwater reservoir), CA	D	C		0.5	11.6	3.0
Miller and Oremland 1988	Western USA meromictic saline lakes	D	C		0.2	77.1	10
Smith and Lewis 1992	Colorado high altitude lakes	D + E	C		0	160	25.6
Barber and Ensign 1979	Lake Wingra (eutrophic)	E	BT	4% to 56%	8.0	3200	16-768
Casper et al. 2000	Priest Pot (hypertrophic)	D	HE		1.0	22.4	5.4
Casper et al. 2000	Priest Pot (hypertrophic)	E	BT	44% to 88%	0	1734	198
Mattson and Likens 1990	Mirror Lake (softwater)	E	BT	70	0.8	68.2	12.2
Fallon et al. 1980	L. Mendota, Wisconsin	D	HE			132	42.1
Baker-Blocker et al. 1977	Michigan ponds	E	BT		92	1100	
Strayer and Tiedje 1978	Wintergreen Lake, Michigan	E	BT	73% to 107%			336
Strayer and Tiedje 1978	Wintergreen Lake, Michigan	D	HE				160-736
Riera et al. 1999	four Wisconsin lakes	D	HE		0.0	320	2.9-19.8
Bastviken et al. 2004	Wisconsin lakes	D + E	C				2.7-70
Michmerhuizen et al. 1996	nineteen Minnesota and Wisconsin lakes	D	HE		2.7	1258	
Striegl and Michmerhuizen 1999	two small Minnesota lakes	D + E	HE,C		1.3	2240	113-150
Varadharajan 2009	Mystic Lake, Massachusettes	E	BT				8-12.8
Arctic							
Kling et al. 1992	N. Alaska Lakes	D	HE		1.3	16.3	6.5
Whalen and Reeburgh 1990	N. Alaska ponds	D	C		4.6	131	21
Bartlett et al. 1992	Yukon-Kuskokwim Delta lakes, Alaska	D	HE		3.8	77.0	13.4-16
Rudd and Hamilton 1978	Canadian Shield Lakes	D	HE		0	960	544
Rudd et al. 1993	Candian Shield Lakes (oligotrophic)	D			0.8	8.3	
Rudd et al. 1993	Canadian reservoirs	D			10.2	20.0	
Roulet et al. 1994	Hudson Bay Lowland pools	D	C				100-163
Hamilton et al. 1994	Hudson Bay Lowland, peatland ponds	D	HE			770	110-180
Hamilton et al. 1994	Hudson Bay Lowland, peatland ponds	E	BT			0	0
Naiman et al. 1991	beaver pond	D + E	C		5.0	200	32-40
Grant and Roulet 2002	beaver pond	E	BT,C,T				100
Grant and Roulet 2002	beaver pond	D	C				91.5
Roulet et al. 1997	beaver ponds	D + E	FG		–70	3240	109
Bastviken et al. 2004	Swedish lakes	D	HE				0.3-7.5
Huttunen et al. 2003	Finnish lakes and reservoirs	D + E	C,BT		5.1	82	
Juutinen et al. 2009	207 Finnish lakes	D	HE				0.14-81
Nakayama et al. 1994	Shallow Siberian alases near Yakutsk	E	SS	38% to 74%			231-528
Zimov et al. 2001	Siberian thermokarst lakes	D	HE		0		7.6
Zimov et al. 2001	Siberian thermokarst lakes	E	BT	>80%			>70
This study	Siberia (Grass L., Shuchi L., Tube D. L)	D	HE				69, 10, 11
This study	Alaska and Siberia thermokarst lakes	E	ICE,BT	73% to 78%	0	25,000	27,450

†Method abbreviated: BT, bubble trap; C, floating chamber; HE, headspace equilibration; T, eddy flux tower; FG, flux gradient technique measuring CH_4 concentration in air at different heights above lake; SS, sediment stirring to release bubbles into inverted funnels; ICE, surveys of bubble clusters on lake ice

among lakes in different regions, we collected gas samples using submerged bubble traps on 133 seeps from 16 lakes in Alaska and Siberia. Bubble gas was collected from traps as soon as enough volume had accumulated for sampling, which was typically several hours to 10 d. We stored samples in the dark at 4°C in clear glass serum bottles sealed with butyl rubber stoppers and aluminum crimp caps until analysis. Methane concentration (by volume) of Siberian samples was determined using a TCD Shimadzu 8A and Alaskan samples using a Shimadzu GC-2014 gas chromatograph fitted with both thermal conductance (TCD) and flame ionization (FID) detectors (analytical error < 1% CH_4).

The biogenic origin of CH_4 in seeps was determined using stable isotope and radiocarbon analyses by Walter et al. (2008a). Here, stable isotope analysis was used to quantify the potential for a sampling artifact to influence determinations of CH_4 concentrations in bubbles. Due to the slow rate of gas accumulation in bubble traps placed over type A seeps, bubble gas held within traps is subject to physical and biological transformation in traps during days to weeks. To determine the potential for CH_4 oxidation of bubble gas in traps, we measured the $\delta^{13}C$ values of CH_4 and CO_2 in type A bubbles held in collection traps for shorter (2-10) and long (25 d) periods. We measured $^{13}C/^{12}C$ of CH_4 and CO_2 by direct syringe injection using gas chromatography/mass spectrometry (Hewlett-Packard 5890 Series II GC coupled to a Finnigan MAT Delta S). Stable isotope compositions are expressed in δ (‰) = 10^3 ($[R_{sample}/R_{standard}] - 1$), where R is $^{13}C/^{12}C$ and standard refers to the Vienna Pee Dee Belemnite (VPDB). The analytical errors of the stable isotopic analyses were ± 0.1% δ ^{13}C.

Long-term methane flux measurements by traditional methods—We made biweekly measurements of diffusive emission throughout the entire open-water period on three Siberian lakes (approx. 4 Jun–4 Oct 2003) using surface water CH_4 concentration determinations on triplicate field samples and the boundary layer model with meteorological assumptions described by Kling et al. (1992). During the period of fall turnover in 2003, measurements were made every 2-4 d. We also sampled dissolved CH_4 concentrations in lake water beneath the ice in early and mid-May 2003.

We made daily measurements of 'background' ebullition in 34 bubble traps using the traditional method of random trap placement within specific zones of the lakes, which in the cases of Siberian lakes, Shuchi L. and Tube Dispenser L., were thermokarst and non-thermokarst margins and deep lake centers. Traps were placed in the center only of Grass L. because the broad floating-mat perimeter prevented distinction of any margin types and because the lake was 10 m deep at the edge of the floating mat. Randomly placed bubble traps were constructed from a weighted copper wire ring (~1 m diameter), woven through a circle of polyethylene film (0.15 mm thick). The center of the polyethylene circle was sealed around the mouth of an inverted polycarbonate bottle. A hole drilled into the top of the inverted bottle allowed the trapped gas to be released through tygon tubing and a stopcock into a graduated cylinder for bubble volume measurement. In lakes, bubble traps attached to ropes were anchored to the lake bottom, kept afloat by 2-L bottles that served as buoys, and permitted to roam around the tethering rope driven by wind and currents. The length of the tethering rope was 1.5 m greater than the lake water depth at each site. We measured the volume of gas accumulated in submerged bubble traps daily from a rowboat in summer and several times per week from the ice in winter. In winter, we accessed bubble traps by carefully penetrating the ice with a pick.

A new technique to quantify ebullition: Selective sampling of discrete seeps—We took advantage of the unique opportunity that northern, seasonally ice-covered lakes provide to quantify the spatial patchiness of bubbling using a new technique. We located point sources of ebullition by removing snow from frozen lake surfaces in early winter to map the locations of bubbles trapped in the ice. Much like a time-lapse photograph, the ice literally froze into place the bubbles that had been produced since ice cover had formed. Ice bubble surveys revealed that bubbles were not randomly dispersed, but occurred in distinct clusters representing discrete ebullition seeps (Table 2).

The Russian term for methane bubble clusters in lake ice is 'koshka,' which translates to English as 'cat,' likely reflecting the resemblance between the bubble cluster patterns and a cat's paw print. Exploiting the richness of the Russian language, which contains many expressions of 'cat,' we named three seep types according to distinct bubble cluster patterns in ice: 'Kotenok' (type A), the weakest of the seep types, translates as 'kitten'; 'koshka' (type B) is a typical 'tomcat', and 'kotara' (type C), implies 'a big, fat grandfather cat that sits on the woodstove.' We identified a fourth ebullition seep class as 'Hotspot' because constant high rates of bubbling maintain relatively ice-free holes (0.3-1 m diameter) above the sediment vent due to the convection of warm (0-2°C) lake water carried to the surface by bubbling.

Placing bubble traps beneath the ice where bubble clusters occurred, we selectively measured ebullition to determine whether or not the four seep classes could be distinguished by temporal bubbling dynamics. Long-term (up to 359 d) measurements on Siberian seeps were made using the submerged manual collection trap described in the traditional methods above. In the interior Alaska lake, we measured long-term (up to 700 d) seep ebullition using an upgraded, automated version of the bubble trap, the design of which is described in detail by Vas et al. (2010). Briefly, the improved bubble trap included a submerged, inverted tipping cup (40-90 mL) and an Onset event data logger for tipping rain gauges and industrial counting (MicroDaq Ltd, part # H07-002-04) to automate measurements in winter beneath thick lake ice. The data loggers counted each time a full cup tipped to release bubble gas, and tipping event records were uploaded onto a laptop computer plugged into a cable snaking through the ice. When low-

Table 2. Classification of ebullition seeps by CH_4 bubble-clusters patterns in lake ice; CH_4 concentrations in bubble gas (% by volume); and summer, winter, and annual ebullition determined by long-term flux measurements. Error estimates (standard error of *n* seeps) represent differences in CH_4 concentrations and ebullition between individual seeps in each category. The lines on the meter sticks in the photos of type A and B mark 10 cm wide intervals.

				Ebullition (mg CH_4 d^{-1})		
	Seep	Description	CH_4 (%)	Summer	Winter	Annual
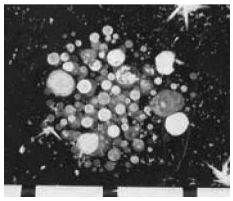	A	Isolated bubbles in multiple ice layers	73 ± 11, *n* = 6	28 ± 19, *n* = 3	8 ± 5, *n* = 8	16 ± 10
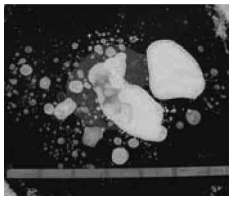	B	Merged bubbles in multiple ice layers	75 ± 3, *n* = 35	210 ± 8, *n* = 2	81 ± 29, *n* = 4	131 ± 30
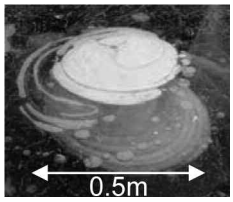	C	Single gas pockets stacked in ice	76 ± 3, *n* = 41	1042 ± 210, *n* = 6	925 ± 98, *n* = 9	971 ± 142
	Hotspot	Relatively open hole in winter lake ice	78 ± 2, *n* = 52	3130 ± 244, *n* = 4	3240 ± 412, *n* = 10	3197 ± 484

flux seeps had less than one tipping event per day, the volume of the tipping cup was averaged across the prior zero-tip days to interpolate the low flux across the measurement period. Cross-calibration of the manual and automated gas collection traps showed agreement. Using the ideal gas law, we converted flux values measured in mL gas d^{-1} to mg CH_4 d^{-1} taking into account the mean partial pressure of CH_4 determined for each seep class from measurements of a large number of seeps sampled in different regions. Ebullition measurements using the manual collection traps were corrected for atmospheric pressure and temperature at the time of volumetric readings. Flux calculations using automated traps accounted for hydrostatic pressure (atmospheric pressure and water column) influence on tipping cup volumes at the time of events. We assessed the potential for short-term flux measurements to reflect long-term mean ebullition for seeps by subsampling ebullition for different measurement periods from the long-term flux data set. We determined mean daily ebullition during the open water (summer) and ice-cover (winter) seasons for each seep as the mean of all daily flux values obtained during those seasons. Descriptions of class-specific bubble patterns and mean annual ebullition expressed as the seasonally weighted mean of all long-term seeps measured in the four categories of biogenic seeps are given in Table 2.

Ice-bubble surveys—To quantify the spatial patchiness of seep ebullition, we calculated an area-based flux by counting the number of seeps in each class along 1 m × 50 m transects on lake ice cleared of snow. Flux values based on the long-term measurements of representative seeps were applied to the distribution of seeps mapped in lake ice to estimate the seasonal and annual emissions on an area-basis along transects. To show that seep categories are recognizable, we introduced the classification system to four new observers and measured the variability among 5 observers, including the author, surveying three transects.

Estimating whole-lake emissions—We estimated whole-lake CH_4 emissions from the three Siberian lakes as the sum of diffusive flux, background ebullition, and discrete seep ebullition

from 4 Jun 2003-1 Jun 2004. Diffusive flux and background ebullition were measured directly on each lake. Missing background flux data in winter on Tube Dispenser L. was accounted for by applying the average of measured winter background emissions from Shuchi L. and Grass L., both of which were close to zero. We estimated discrete seep ebullition by applying mean daily fluxes from long-term measurements of each seep category to the measured density of A, B, C, and Hotspot seeps along six 50 m long on-ice transects in Shuchi L. and Tube Dispenser L. and three transects on Grass L. Results are presented as daily CH_4 release; however, it should be noted that during the ice-free season (approx. 1 Jun-4 Oct in Siberia) CH_4 was released directly to the atmosphere, while in winter, dissolved gases were stored under the ice and much of the ebullition bubbles were trapped in and beneath the ice. During spring-ice melt, we observed CH_4 release from disintegrating ice pockets on all lakes.

Application of method to other arctic and sub-arctic lakes—To demonstrate the relevance of this method to understanding lake CH_4 emissions, we conducted ice-bubble surveys on early winter lake ice in Siberia and near Toolik Field Station, Alaska— regions where lake CH_4 emission estimates had been made in the past using traditional methods (Zimov et al. 1997; Kling et al. 1992). To determine within-lake variability in CH_4 ebullition, we surveyed along 2-6 transects per lake on nine lakes, in the littoral, transition, and pelagic zones of each lake. In lakes where more than one shore type was observed, for instance the thermokarst and non-thermokarst shore types of Siberian lakes, we conducted transects along each shore type. Seep ebullition emissions measured along transects were extrapolated to entire lakes based on the fraction of the lake that each measured zone occupied according to bathymetry and ice bubble observations. In the non-thermokarst lakes near Toolik Field Station, we estimated whole lake seep ebullition emissions as the mean of all transects.

Finally, to test the hypothesis that including estimates of CH_4 emitted from lakes, based on the technique introduced in this article, would significantly increase prior model estimates of regional emissions that ignored lakes, we ran a modeling experiment with the Terrestrial Ecosystem Model (TEM) on 74 grid cells in NE Siberia at a resolution of 0.5° × 0.5° (Zhuang et al. 2004).

Statistics—We assessed statistical differences in bubble CH_4 concentration and flux among ebullition seep classes and study lakes using two-way ANOVA. We used linear regression analysis to test the potential relationships between individual seep flux and bubble cluster area within seep classes, and log-transformed ebullition versus the fractions of transects covered by bubble clusters. All statistical analyses were conducted in SAS 9.1.

Assessment

Isotopic values of CH_4 determined from type A bubbles held in collection traps for 25 d ($\delta^{13}C_{CH4}$ –59.7 ± –2.9 ‰, n = 5 samples) were on average 19% more enriched in $\delta^{13}C$ than bubbles collected from traps within 2-10 d ($\delta^{13}C_{CH4}$ –69.7 ± 1.9 ‰, n = 8 samples; Fig. 1). Similarly, bubble CO_2, one of the two products of CH_4 oxidation, was 21% more depleted with respect to $\delta^{13}C$ than CO_2 in bubble gas collected over a shorter period.

Methane concentration varied among the seep classes and between lakes (ANOVA, $F = 21.48_{34,99}$, $P < 0.0001$). Fig. 2 shows the CH_4 concentrations measured in gas sampled from 133 ebullition seeps in 16 lakes in different regions of Alaska and Siberia. Bubble gas collected from type A seeps had the lowest CH_4 concentration and largest variability among the four classes of seeps (mean ± standard error; n, number of samples): A, 59 ± 9% CH_4, n = 6; B, 69 ± 3% CH_4, n = 35; C, 70 ± 3% CH_4, n = 41; HS, 78 ± 2% CH_4, n = 52. Repeated measurements from individual seeps showed temporal variability in CH_4 concentration ranging from 20% to 30% for Type A (standard deviation/mean), 12% to 23% for Type B, 2% to 39% for Type C, and 0% to 12% for Hotspots. Final CH_4 concentrations for each seep class (A = 73 ± 11%; B = 75 ± 3%; C = 76 ± 3%; and HS = 78 ± 2%) were derived by applying a 20% correction factor to Type A seep concentrations to account for CH_4 converted to CO_2 (see isotopic data) during the average holding day period of 6 d, an 8% correction factor for Type B and C seeps, which were typically held in traps for 2-3 d, and no correction factor for Hotspot seeps, from which gas was typically collected within 2-6 h of trap placement.

Analysis of long-term flux data revealed differences in ebullition rate among the four seep classes (ANOVA, $F = 41.19_{7,53}$, $P < 0.0001$; Table 2), but the differences were unrelated to the lake, region, or season in which they were measured. We found no significant relationship between ebullition from individual seeps and the size of their bubble clusters in lake ice. Averaging all long-term daily flux values obtained for indi-

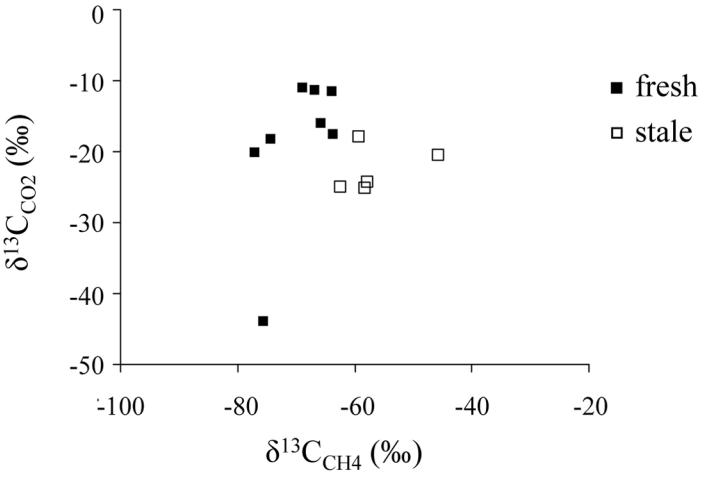

Fig. 1. The $\delta^{13}C_{CO2}$ and $\delta^{13}C_{CH4}$ of Type A bubble gas stored in gas collection traps in Alaskan lakes over periods of 2-10 d (fresh) and 25 d (stale). Typically, gases collected from higher flux seeps (B, C, Hotspot) accumulated more quickly, allowing for sampling within 1-72 h.

vidual seeps within classes by day of the year, we determined mean daily seep-class ebullition to show differences among classes (Fig. 3). Seasonal ebullition was calculated for each seep class as the mean and standard error of individual seeps measured across both summer (open water) and winter (ice cover) seasons (Table 2). Scaling mean daily fluxes for each seep to 365 d of the year based on 142 d of open water summer season (mean number of days observed on Alaskan and Siberian study lakes), we found that the mean annual ebullition for each seep class was as follows: A, 6 ± 4 g CH_4 y^{-1}, n = 8 seeps; B, 48 ± 11 g CH_4 y^{-1}, n = 4 seeps; C, 354 ± 52 g CH_4 y^{-1}, n = 9 seeps; Hotspot, 1,167 ± 177 g CH_4 y^{-1}, n = 10 seeps.

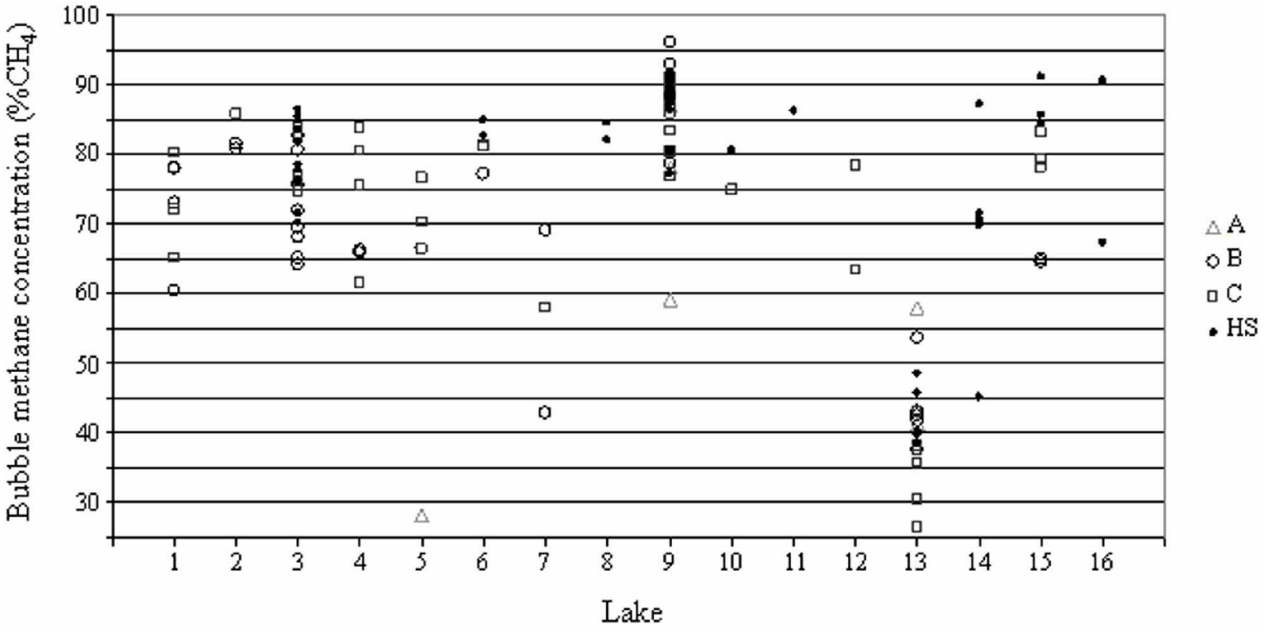

Fig. 2. Methane concentration measured in type A, B, C, and Hotspot seeps in different regions of Alaska and Siberia: Lakes 1-6 (Northern Seward Peninsula, Alaska); lakes 7-8 (North Slope of Alaska's Brooks Range); lakes 9-14 (Interior Alaska); lakes 15-16 (Kolyma Lowland, Siberia).

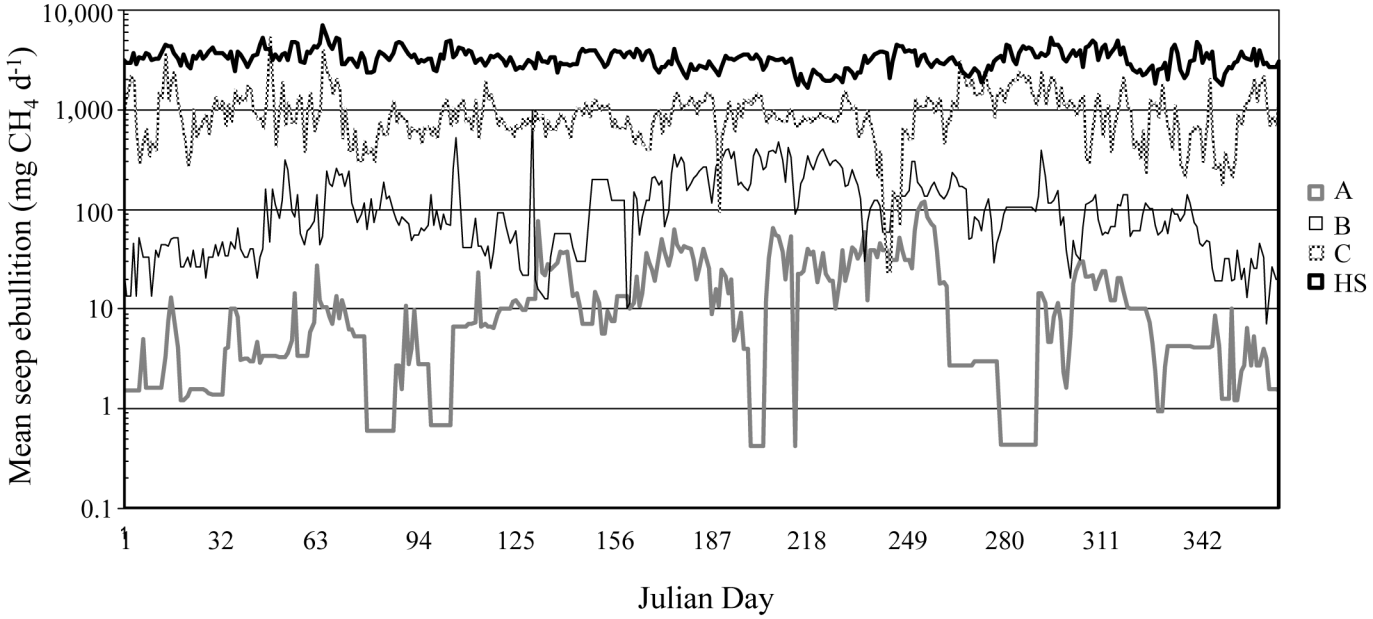

Fig. 3. Mean daily ebullition of biogenic seeps types A, B, C, and Hotspot (HS) as the average of all long-term ebullition values (4-10 seeps per class) measured on each Julian Day in Siberia and Alaska. Data were interpolated across 2/29 on non-leap years. Ebullition data are presented on a log-scale on the Y-axis.

Short-term field measurements (hours-days) of ebullition are common, particularly in remote study sites where long-term monitoring of seep ebullition is not feasible. Analysis of our continuous, long-term measurements of individual seeps revealed that ebullition was highly variable over periods of hours to days. The standard deviation was much larger than the mean of short-term measurements for all seep classes except hotspots (Fig. 4). The relative error (SD/mean) of the A seep in Fig. 4 was as high as 225% for daily ebullition, whereas measurements over 300 d had relative error of only 10% for the same seep. The temporal variability due to seep response to fluctuations in atmospheric pressure was apparent in all seep classes. The fraction of the daily ebullition data that fell within 10% of the long-term mean for individual seeps in Fig. 4 was 7% to 29%. These results suggest that short-term flux measurements are unlikely to represent the long-term mean emission from seeps and should be used with caution in other studies.

Description of seep classes—Type A seeps are characterized by the lowest fluxes (16 ± 10 mg CH_4 d^{-1}), which produce patterns in winter lake ice recognized as isolated bubbles stacked in multiple layers of ice. The layering of ebullition bubbles in ice represents repeated ebullition events. Individual bubbles within the cluster typically range from 0.5-3 cm in diameter. The cluster of bubbles comprising an A seep pattern is typically under 40 cm in diameter; however, bubble density within clusters is variable. Occasionally small A-type seeps contain some merged bubbles, but the merging should be less than 50% of all bubble gas volume to distinguish them from type B seeps.

Type B seeps, which emit 131 ± 30 mg CH_4 d^{-1}, produce patterns in ice in which merged bubbles dominate, and occur as stacks in multiple layers of ice. Merged bubbles, which appear as bubbles trapped during active coalescence or as bubbles larger than 10 cm in diameter constitute more than 50% of all bubble gas volume. Bubble cluster diameter is typically > 30cm.

Type C seeps are recognized in ice bubble surveys as single, large pockets of gas (generally >40 cm diameter) with smooth edges and relatively few (under 25%) isolated bubbles around

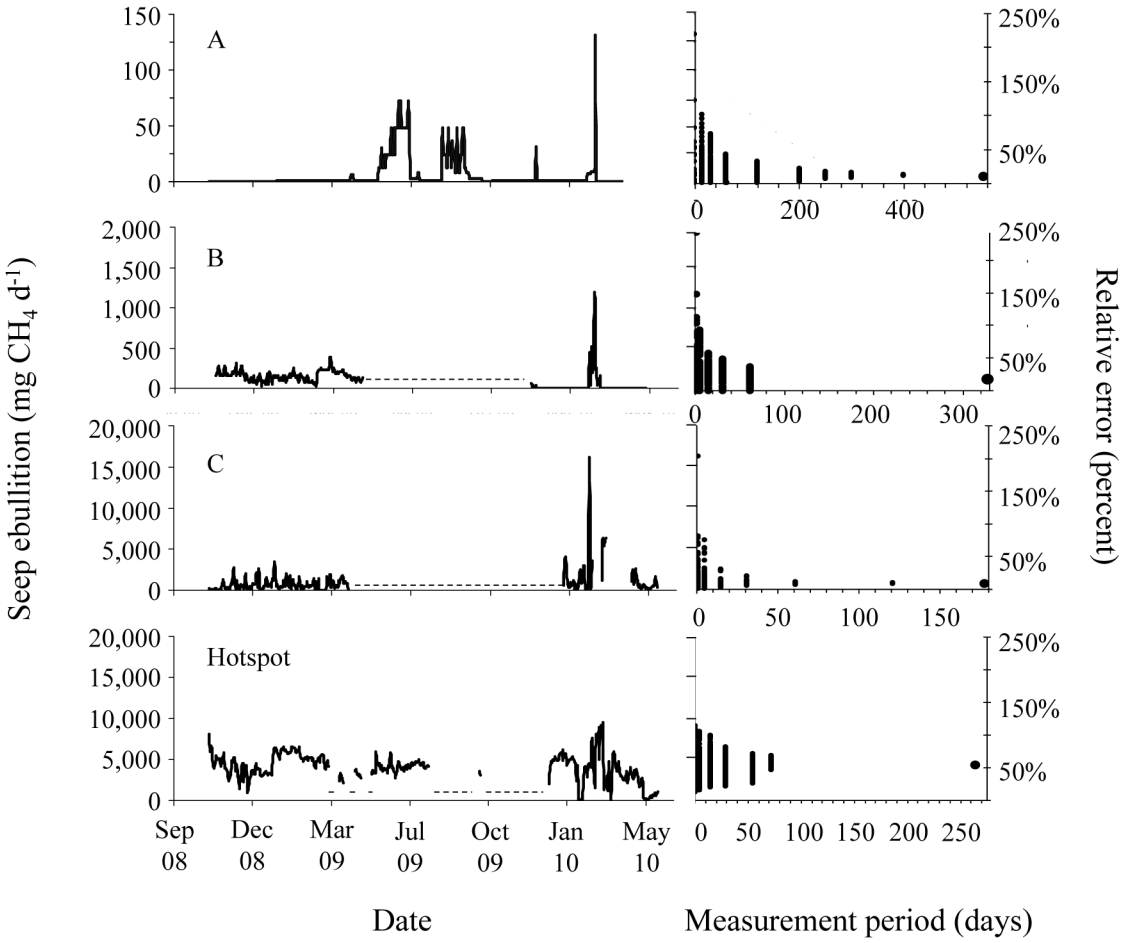

Fig. 4. Mean daily ebullition measured from Aug 2008-May 2010 for individual A, B, C, and Hotspot seeps on an Alaskan lake (left), and the distribution of measured ebullition values as a function of measurement period (right). The scale of the Y_1-axis differs for A, B, C, and Hotspot examples. Relative error of ebullition (standard deviation/ mean) was inversely related to period of measurement (dotted line; Y_2-axis). Over short periods of measurement, ebullition from individual seeps was highly variable suggesting that such that short-term flux measurements are unlikely to represent the long-term mean emission from seeps. Periods of no data are indicated by a dashed line on the left-side panels.

the edge. Large pockets are often stacked on top of one another, with up to several decimeters of ice separating pockets vertically. During ebullition events, fluxes from C-type seeps are typically indistinguishable from the flux of Hotspots; however, C-seep ebullition is intermittent. Bubbling episodes tend to last 7-10 d, separated by 1-4 d of zero or near-zero flux, during which lake ice thickens and encapsulates the large pockets of gas already released. The long-term daily mean flux of C seeps was 971 ± 142 mg CH_4 d^{-1}.

Hotspot seeps had the highest mean daily ebullition due to nearly continuous high-rates of ebullition (3197 ± 484 mg CH_4 d^{-1}). In early winter, hotspots are recognized as open holes in lake ice, with bubble release episodes occurring as often as every 0.1-3 min. Over time, decline in atmospheric temperature, lake-ice thickening, and the accumulation of snow or snow-ice on lake surfaces can 'cover' hotspots. While gas may escape from all seep types in early winter following a heavy snow, from which the overburden pressure forces lake water up through the weak ice lenses separating bubbles, hotspot seeps are most likely to emit gas year round through the ice. We observed the build-up and release of gas through microcracks in the ice over some hotspots in winter. Hotspots were also easily opened at all times of year by prying with an ice pick. Often prying led to the sudden release of a huge volume of flammable gas (Fig. 5). When ignited in March, the gas from seeps produced flames that we observed for up to 8 and 15 min on lakes in Alaska and Siberia, respectively.

Importance of discrete bubbling seeps in whole-lake CH_4 emissions—Methane ebullition measured by collection traps placed over discrete seeps (16–3197 mg CH_4 d^{-1}, Table 2) was greater than the daily mean of background ebullition (7.4 ± 0.6 mg CH_4 m^{-2} d^{-1}, n = 34 traps) measured through the random placement of traps within specific zones of Siberian thermokarst lakes. Comparing the area of the lake that randomly placed traps covered (<0.03%) to the area of bubble clusters in ice (0.2% to 21% of the lake area depending on the zone of the lake), we found that the probability of randomly placing a trap over a seep was extremely low (6.4×10^{-3} to 5.3×10^{-5}). Because the flux rates measured by these two types of sampling did not overlap, and because the probability of randomly placing a bubble trap over a discrete seep was consistently low, we calculated whole-lake emissions as the sum of diffusive fluxes, background bubbling (measured using randomly placed bubble traps), and bubbling through discrete seeps.

The importance of seep ebullition varied among lakes (Fig. 6). Seep ebullition comprised 87% and 86% of whole-lake CH_4 emissions from Shuchi L. and Tube Dispenser L., respectively. Molecular diffusion accounted for 5% and 4%, whereas background ebullition was 8% and 11% for the lakes, respectively. CH_4 emission from Grass L. was lower than from the active thermokarst lakes, and consisted of 30% seep ebullition, 7% background ebullition, and 63% diffusion.

Seep ebullition also varied among zones within the lakes (Fig. 7). Emission from seeps was 93% of total emissions from the thermokarst zone in Shuchi Lake, but only 9% from the non-thermokarst margins and 31% from the lake center.

Fig. 5. The release and ignition of CH_4 from an ice-bubble pocket on an Alaskan lake in November 2009. UAF photo by Todd Paris.

Results of the ice bubble surveys revealed that ebullition seeps occurred along transects on all six Alaska tundra lakes surveyed near Toolik Field Station, but their abundance differed among lakes and transects (Fig. 8). Applying the mean daily CH_4 flux associated with each seep class to the distribution of seeps surveyed on Alaskan tundra lakes in October 2004, we estimated an average daily bubbling of 27 ± 10 mg CH_4 m^{-2} of lake (mean ± SE, n = 6 lakes). To estimate the average annual regional emission from lakes near Toolik, we weighted the contribution from each of the six lakes by the fraction of its area relative to the total area of all six lakes, and extrapolated daily seep CH_4 fluxes to 365 d per year (5.6 g CH_4 m^{-2} of lake area y^{-1}).

The relative error in estimated seep ebullition from transects due to differences in classifying seeps as A, B, C, or Hotspot among five independent observers was 9% to 11%.

We found a positive relationship between log-transformed ebullition along transects and the area that bubble clusters occupied on all transects ($F = 24.8_{1,25}$, $P < 0.001$; R^2_{adj} = 0.5; Fig. 8).

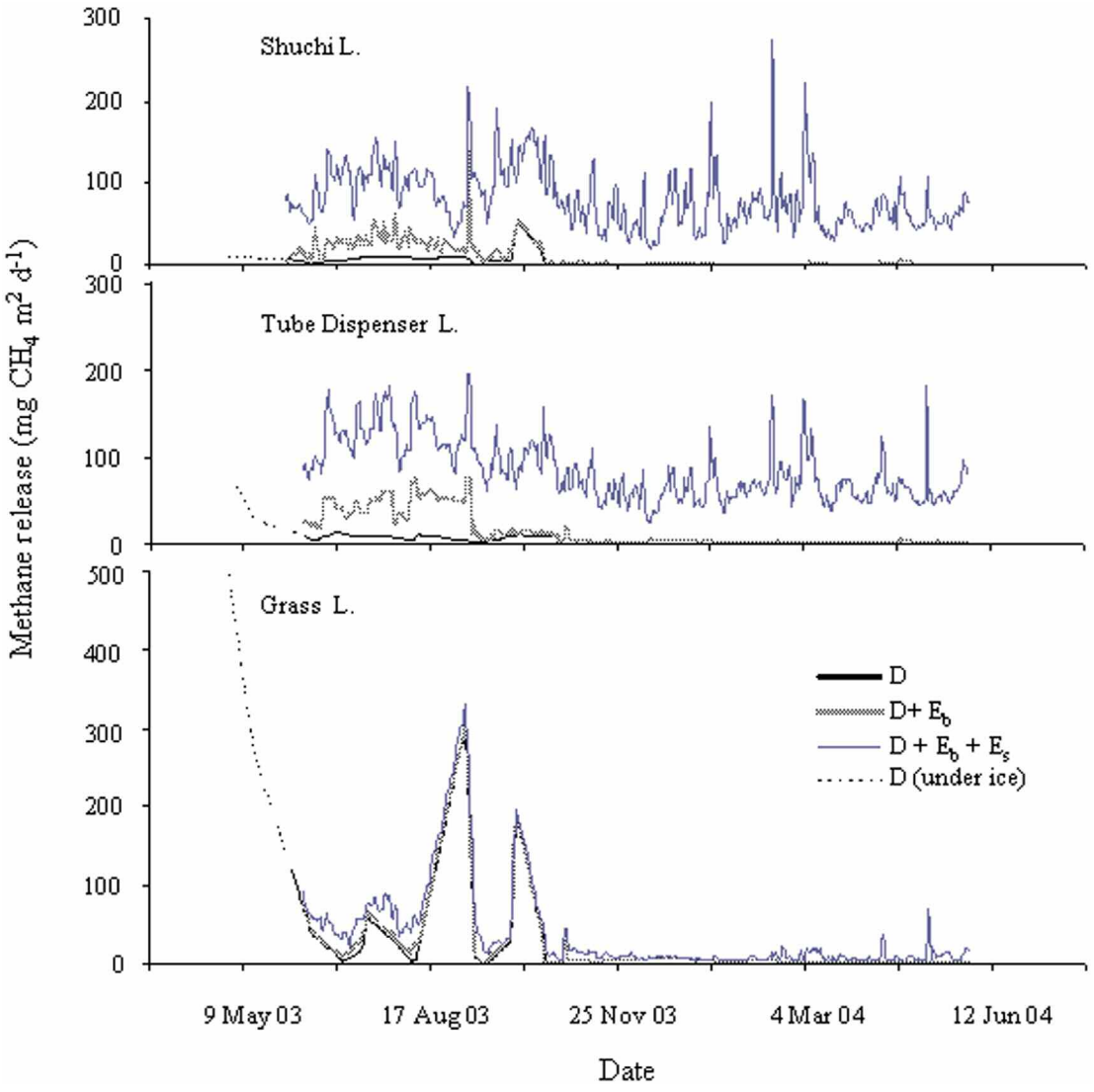

Fig. 6. Methane release by diffusion (D), background ebullition (Eb), and seep ebullition (Es) shown as cumulative flux in three Siberian lakes: Shuchi (top), Tube Dispenser (middle), and Grass (bottom). During the ice-free season (approx. Jun 1-Oct 9) gas is released directly to the atmosphere. During the ice-cover season, the majority of CH_4 is trapped as dissolved gas (dotted line) beneath the ice or as bubbles pockets in the ice.

Implications for bottom-up biogeochemical modeling—Given the difficulties of quantifying the patchiness of ebullition in the past and the paucity of studies that synthesize lake ebullition as a source of atmospheric CH_4, lake contributions have, until now, been considered negligible in the global atmospheric CH_4 budget. Consequently, lake processes have not been incorporated in biogeochemical models that simulate CH_4 emissions from northern wetlands, such as the Terrestrial Ecosystem Model (TEM) (Zhuang et al. 2004). When included in the TEM, we found that seep emissions derived by the ice-survey method introduced here significantly increased estimates relative to prior model estimates of regional emissions in Siberia that ignored lakes. Adding the CH_4 emission estimate from North Siberian yedoma lakes as the mean annual emissions from Shuchi L., Tube Dispenser L., and Grass L. (25 ± 5 g CH_4 m^{-2} of lake y^{-1}) to the regional net CH_4 emissions estimated by TEM for a fraction (80,636 km^2) of the $1x10^6$ km^2 ice-rich loess region of Northeast Siberia, increased the regional flux estimate 3- to 7-fold from 0.1 Tg CH_4 y^{-1} to 0.3-0.7 Tg CH_4 y^{-1}. The range reflects variation in estimates of lake area (10% to 30% lake area) for North Siberia (Mostakhov 1973; Zimov et al. 1997; Walter et al. 2006).

Protocol for lake-ice methane bubble cluster survey—Quantifying the abundance and distribution of methane seeps in lakes is best done in early winter on hard black ice as soon as lake ice is thick enough to walk on (at least 10 cm ice thickness). Additional details on ice safety are provided by the U.S. Army CRREL (1999). Early winter surveys have several advantages. Shortly after ice formation, ice thickness is relatively uniform across the lake surface, resulting in a more accurate picture of

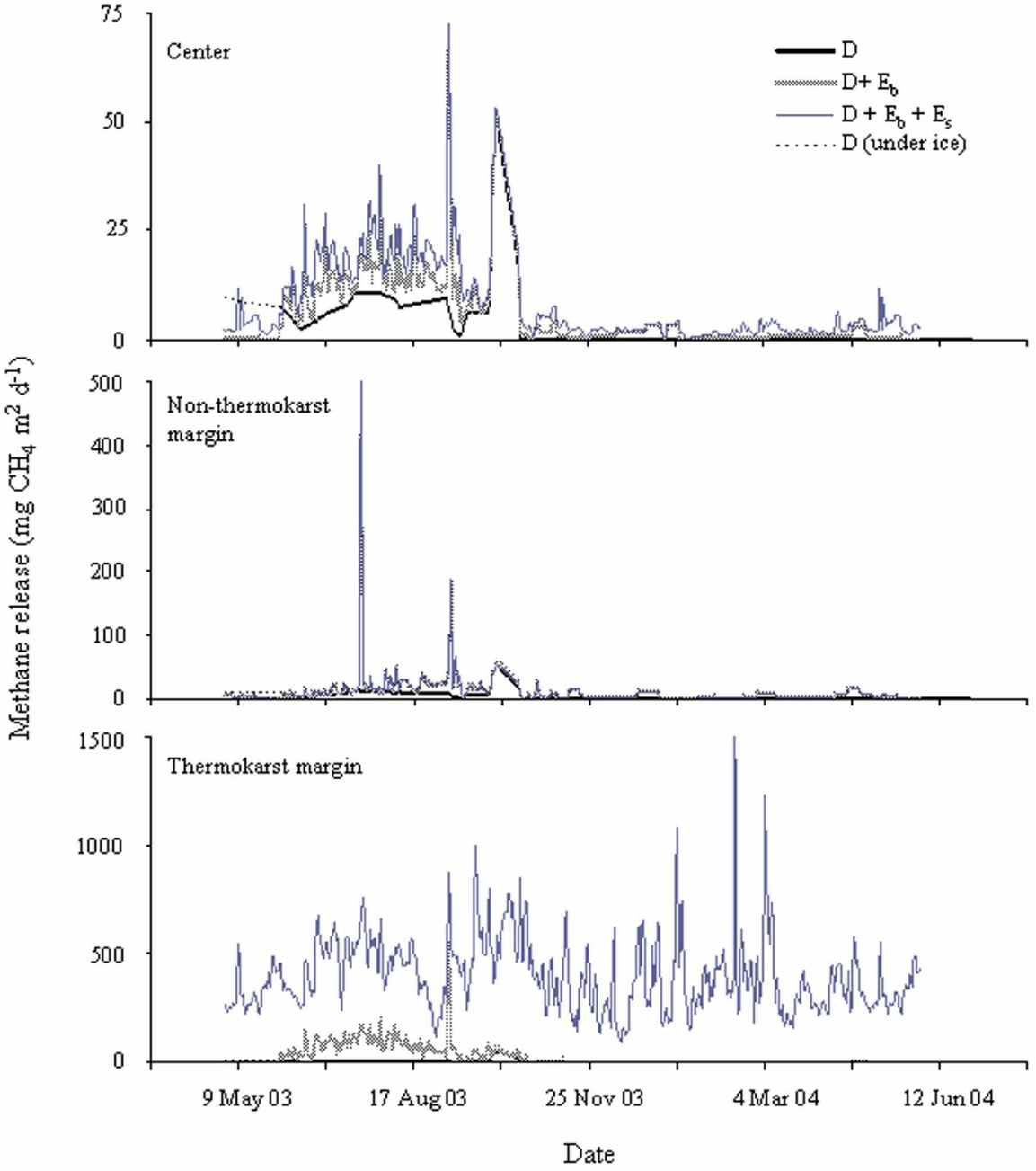

Fig. 7. Methane release by diffusion (D), background ebullition (E_b), and seep ebullition (E_s) shown as cumulative flux from different zones within Shuchi Lake: center (top, 79% of lake area), non-thermokarst margin (middle, 3% of lake area), and thermokarst margin (bottom, 18% of lake area). During the ice-free season (approx. Jun 1-Oct 9) gas was released directly to the atmosphere. During the ice-cover season, the majority of CH_4 was trapped as dissolved gas (dotted line) beneath the ice or as bubbles pockets in the ice. Y-axes in the panels have different scales to emphasize the between-zone variability in D, E_b, and E_s. Daily diffusion emissions were estimated by assuming a linear relationship between measurements every 2-14 d.

the precise number and locations of methane seeps. Little or no snow cover on lakes minimizes effort required to clear snow from transects, and conducting surveys prior to heavy snow fall reduces the likelihood of opaque, white-ice formation on lakes. This field method is simple and requires few, inexpensive field supplies: flat-bottom snow shovel, broom, ice pick (motorized auger is optional), 5-gallon bucket, waterproof gloves, 1-m measuring stick, 50-m measuring tape, depth sounder, digital camera, GPS, field notebook, and pencil.

Step-by-step instructions for surveys include the following:

1. At each lake, mark the location of desired transects using a GPS. Hand-drawn sketches in a field notebook of the lake and orientation of transects relative to different types of shorelines, roads, buildings, etc. are helpful for reference.

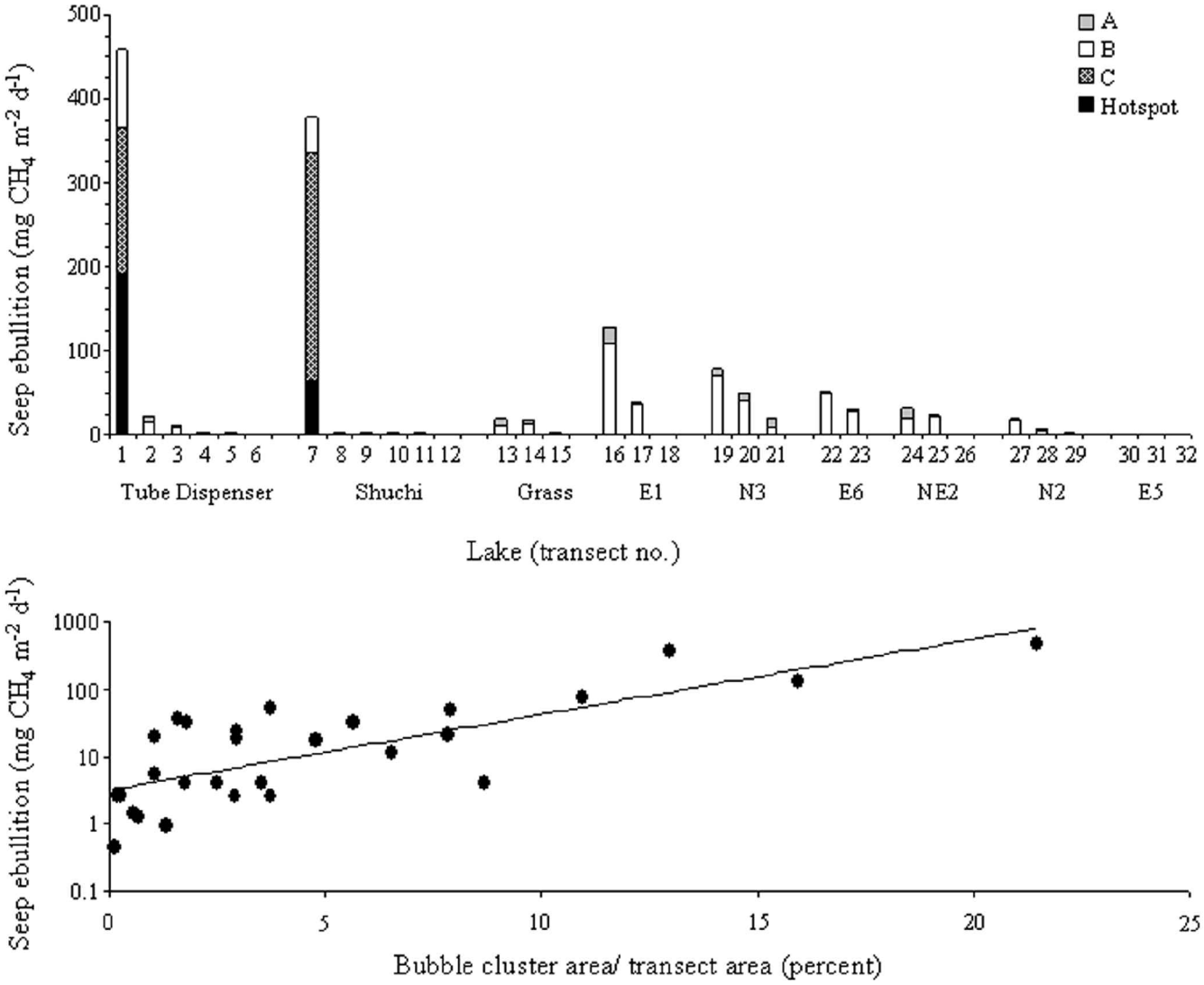

Fig. 8. Contributions of A, B, C, and Hotspot seeps to total seep ebullition along transects surveyed in early winter lake ice on three Siberian lakes (Tube Dispenser, Shuchi, Grass) and six tundra lakes near Toolik Lake Field Station (E1, N3, E6, NE2, N2, E5) (top), and the relationship between fraction of the ice covered by bubble clusters and ebullition along 28 transects containing seep ebullition bubbles (bottom). Transects 1 and 7 along the thermokarst margins of Tube Dispenser and Shuchi lakes had exceptionally high CH_4 emissions from ebullition seeps.

2. Using a flat-bottom shovel, broom, and measuring tape, remove the snow from transects 1-m wide by 50-m long. We found that the density of seeps within zones of lakes is well represented on scales of several tens of meters, and therefore suggest a minimum transect length of 50 m.
3. Open a hole in the lake ice with a pick or auger wide enough to submerge a 5-gallon bucket adjacent to the transect.
4. Fill and pour buckets of lake water onto the snow-free transect to improve transparency of lake ice for detecting bubbles.
5. Starting at one end, walk the transect with a GPS and meter stick, recording the size (width × length) and class (A/B/C/Hotspot, or 'none') of each bubble cluster that falls within the 1-m width of the transect. Mark the location of each seep with a GPS. If a cluster is partially inside the 1-m width, note the dimensions of the portion that falls within the transect only, and indicate '*' for partial seeps in the field notes. Partial seeps are counted as half the flux value of full seeps when scaling up. If bubbles do not occur in multiple layers but only in one distinct layer, then record the class as 'none' along with the dimensions of the bubbles. The lack of repeated bubbling at this location is assumed to indicate that this is not a true seep. "None" bubbles are likely what contribute to background bubbling captured through random placement of traps in most stud-

ies. If there are many seeps in the lake ice along a transect, a long list will be generated. Data lists will look something like this:

Transect 1

GPS waypoint	Length (cm) × width (cm)	Type
1	20 × 20	A
2	10 × 10	A
3	15 × 20	A
4	50 × 50	C
5	30 × 45	B
6	30 × 30	B*
7	5 × 5	none
8	10 × 10	A
9	50 × 50	hotspot

6. The ice may not be transparent if it was snowing at the time of freeze-up or if overflow water from the lake spilled out onto the ice surface, mixing with snow and freezing as solid white ice. In these cases, it may be impossible to see into the lake ice to discern ebullition bubbles. The area of the transect with opaque ice must be measured, noted, and eventually subtracted from the transect survey area.
7. For later interpretation of between-lake and within-lake variability in CH_4 emissions, make field notes and photograph potentially important environmental factors such as:
   a. Ice conditions [clear black ice, opaque white, or yellow ice, wet slush, cracks in ice (big/small; many/few)]
   b. Lake water color (clear, brown, other)
   c. Odor (none, H_2S, organic matter decay)
   d. Lake margin observations (steep versus gradual, erosion, emergent plants, floating mats)
   e. Presence/absence of submerged aquatic plants visible beneath ice and their often associated tiny photosynthesis bubbles visible around plant tissues. Photosynthesis bubbles are quite distinct from true ebullition. They are tiny (<3mm), relative to ebullition (usually >1cm), and occur in dense clusters around frozen plant tissues, similar in appearance to cotton candy. The presence of aquatic plants is noteworthy for consideration of CH_4 emissions through emergent plants, and in that, senesced plant materials may provide an organic substrate for fermentation and methanogenesis in lake sediments. Furthermore, the presence of photosynthesis bubbles in lake ice should be noted because they can be distinguished from ebullition bubbles in ice using particular beam modes of Synthetic Aperture Radar (M. Engram pers. comm.).
   f. Depth of lake water over which the transect was studied

Fresh gas samples may be collected from ebullition seeps by deploying bubble traps beneath the ice over the seeps. The cost of materials is estimated at under $15.00 per trap in the United States, and individual traps can be constructed in 30 min. Gas trapped within the ice can also be collected by carefully creating a shallow pool of water in the ice above the gas pocket, then puncturing a hole in the ice lens to allow bubbles to stream up through the ice into an inverted, water-filled glass vial. Bubbles displace water in the vial. Inverted vials are sealed with butyl rubber stoppers under water to prevent atmospheric contamination and brought back to the laboratory for analysis.

To calculate the flux of CH_4 through seeps, multiply each recorded seep on a transect by the fluxes in Table 2, then divide by the total area of the transect surveyed. Measured CH_4 concentrations of fresh bubbles can be applied together with atmospheric temperature and pressure to the Ideal Gas Law to convert volumetric flux measurements to flux in mg CH_4 m^{-2} d^{-1}.

Discussion

Seep ebullition is an important component of whole-lake CH_4 emissions, and if accounted for, could significantly increase estimates of regional lake emissions. We demonstrated this by determining that seeps were ubiquitous among the Siberian and Alaska lakes we surveyed; that it dominated total lake emissions in some lakes; and, that including ebullition-seep emissions in a biogeochemical model greatly increased observation-based estimates of regional CH_4 emissions in Siberia.

To evaluate the importance of ebullition seeps, we compared CH_4 emission estimates derived from bubble cluster surveys on lake ice (this new method) with previous estimates for lakes from the same regions that ignored discrete seeps. Kling et al. (1992) estimated ~24 g C m^{-2} y^{-1} from lakes, of which 0.5 g C-CH_4 m^{-2} y^{-1} was from diffusive flux of CH_4 and 23.5 g C m^{-2} y^{-1} was CO_2 diffusive flux. Assuming that the six tundra lakes that we sampled were representative of lakes in the region near Toolik Lake Field Station, then adding seep ebullition (5.6 g CH_4 m^{-2} lake y^{-1}) increased the earlier diffusion-derived regional estimate of summertime CH_4 emissions from lakes of 0.67 g CH_4 m^{-2} of lake y^{-1} by 8-fold. Accounting for seep CH_4 adds an additional 17% (4.2 g C-CH_4 m^{-2} y^{-1}) to the total C release from the Toolik Lake area lakes based on Kling et al.'s (1992) regional C budget for lakes. It also increases the total CO_2 equivalents for these lakes, taking into account the Global Warming Potential of CH_4 (25), 2.4-fold, from 103 g CO_2-eq m^{-2} y^{-1} to 242 g CO_2-eq m^{-2} y^{-1}.

For the three intensively studied lakes in Siberia, we conclude that adding seep ebullition (4 g CH_4 m^{-2} lake y^{-1}, Grass; and 26 g CH_4 m^{-2} lake y^{-1}, Shuchi L. and Tube Dispenser L.) yielded a 1.5- and 8-fold increase respectively in total lake emissions to the estimate that would be derived by only reporting diffusion and background ebullition. These results are similar to the ~5-fold increase above previous estimates reported by Zimov et al. (1997) for measurements made by traditional methods at Shuchi L. and Tube Dispenser L. in the early 1990s.

The differences in seeps based on ice bubble patterns and corresponding ebullition that have been demonstrated here provide a powerful platform for quantifying CH_4 ebullition

emissions from a large number of lakes by mapping seeps in winter ice. The consistency we found in seep ebullition by class, regardless of year, lake, region, and water depth suggests that this method could be applied to other lakes outside this study. Adding lake CH_4 emissions derived from this study to TEM in the Kolyma Lowland region increased total terrestrial ecosystem emissions 3- to 7-fold, suggesting that if ebullition is ubiquitous among northern lakes, then incorporating lake CH_4 emissions into models like TEM will have important implications for understanding ecosystem greenhouse gas emissions throughout the Arctic.

Improvements upon previous work—Before the availability of long-term measurements on a large number of seeps within each class, Walter et al. (2006) estimated whole-lake emissions based on replicated seep measurements over a 21-d period in Siberia. Ebullition seep class emissions were (mean ± standard error of *n* measurements): A, 25 ± 5 mg CH_4 d^{-1}, $n = 6$; B, 190 ± 61 mg CH_4 d^{-1}, $n = 8$; C, 825 ± 131 mg CH_4 d^{-1}, $n = 7$; and HS, 2175 ± 378 mg CH_4 d^{-1}, $n = 10$. Calculations of ebullition were based on a limited number of measurements from only three seep classes combined: (B, C, Hotspot, 79.6 ± 1.1% CH_4, $n = 36$ measurements), and the assumption of constant atmospheric pressure. The current study has improved upon the method introduced by Walter et al. 2006 by providing long-term measurements on a larger number of seeps in different regions of the Arctic, by accounting for variability in CH_4 concentration within bubbles from 16 lakes, and by using records of atmospheric and hydrostatic pressure to more accurately calculate the moles of CH_4 contained within measured volumes of bubble gas. Long-term ebullition results for the seep classes presented here (Table 2) were 36% and 31% lower than As and Bs in Walter et al. (2006), and 18% and 47% higher than their previous C and HS flux estimates. Due to the longer measurement period, increased number of seeps monitored and diversity in lake regions studied, the revised flux estimates presented here are more applicable to ice-bubble surveys on northern lakes.

Uncertainties and limitations—We quantified various sources of uncertainty associated with the method and its application to northern lakes (Table 3). In order from lowest to highest, uncertainty factors included: (1) misrepresentation of seep class by ice-bubble patterns due to short-term flux dynamics, (2) variability among observers in identifying and classifying seeps on lake-ice bubble surveys, (3) the concentration of CH_4 in ebullition bubbles, (4) within-seep class variability in ebullition, and (5) variability in ebullition among different lakes and (6) among different zones within the same lakes. Method-related uncertainty factors (1-4) were lower than those associated with application of the method in different ecological settings (5-6). This suggests that the greatest challenge in applying this method to lake ecosystems is the selection of lakes and zones within lakes for conducting ice bubble surveys. Whereas current application of the method is limited to researchers physically observing bubbles on lakes, the positive relationship we found between ebullition and seep bubble density on 28 transects on the nine Siberian and Alaskan lakes surveyed (Fig. 8) suggests that application of this method as a means of ground truth to aerial and remote sensing detection and quantification of CH_4 could help resolve the larger spatial challenges of assessing seep ebullition at scales larger than transects within lakes. Pilot results by Walter et al. (2008b) showed that CH_4 ebullition bubbles in ice were detectable by remote sensing Synthetic Aperture Radar analysis. New investigations are underway to improve seep-CH_4 quantification capabilities by understanding SAR signal interactions with CH_4 bubbles, determining sensitive SAR observation parameters, and establishing statistically significant models (Grosse et al. 2008).

Weather-related factors and the timing of surveys have the potential to cause misrepresentation of seep classes by ice-bubble patterns in early winter. Long-term flux monitoring of seeps revealed that 26% of Hotspots and Cs were misclassified originally based on patterns of bubbles in ice. Five of the six instances were C seeps originally classified as Hotspots. Ebullition monitoring of those seeps revealed intermittent zero and near-zero fluxes over the long term, distinguishing the seeps as C types instead of Hotspots. In only one case, an A was mis-

Table 3. Uncertainty factors in constraining ebullition seep contributions to lake CH_4 emissions ordered from lowest to highest. Relative error is the standard deviation/ mean.

Uncertainty factor	Relative error	*n*
Ice-bubble pattern misrepresentation	0.05-0.26	10-12 seeps per class, 4 classes
Observer seep identification	0.09-0.11	5 observers on 3 transects (54-78 seeps per transect)
Bubble CH_4 content	0.19-0.37	6-52 seeps per class, 4 classes
Ebullition within seep classes	0.30-1.31	4-10 seeps per class, 4 classes
Flux among lakes		
(thermokarst lakes)	<0.01	2 lakes
(other lakes)	0.91	7 lakes
Flux among zones within lakes		
(thermokarst lakes)	2.2-2.3	3 zones per lake, 2 lakes
(other lakes)	0.24-1.73	2-3 transects per lake, 7 lakes

classified originally as a B. Despite the relative rarity of C and Hotspot seeps on transects (6% of seeps on 28 Alaskan and Siberian transects in this study), relative to A and B seeps (94%), misidentification of C and Hotspots could have substantially larger impacts on total emission estimates given the large fluxes associated with those seep types.

Weather influences ice bubble patterns largely by the relationship between atmospheric pressure and ebullition. Ice formation following a sustained period of high atmospheric pressure could result in relatively fewer bubbles in ice because ebullition is suppressed during high pressure periods (Mattson and Likens 1990; Vas et al. 2010). Conversely, a low-pressure event following a sustained high pressure system would be recorded as a large volume of bubbles in the ice, potentially causing an overestimate of seep strength in ice-bubble surveys. The timing of ice bubble surveys relative the growth rate of ice is also important for accurate seep identification. In environments, such as the Arctic and sub-Arctic, where lake ice forms relatively quickly due to cold atmospheric temperatures, the likelihood of seep misclassification is indirectly related to lake ice thickness. The short time segment represented in the ice bubble patterns in thin ice may not reflect the long-term ebullition dynamics for seeps. Analysis of short-term flux measurements in our long-term data sets elucidated the problem of high variability in short-term flux measurements (Fig. 4). Accuracy of ice bubble classification is improved if surveys are conducted several weeks to months after ice formation to allow seep ebullition dynamics for each seep type to be adequately expressed in ice. However, the risk with waiting for the ice to thicken is that heavy snow fall on thin ice can cause overflow and refreezing of slush, making ice surveys impossible through the resulting opaque, white ice. Furthermore, due to their insulatory qualities, redistributed snow and accumulated gases in ice eventually lead to uneven ice thickness and microtopography on the bottom side of lake ice. It is possible that these conditions could influence the migration route of bubbles beneath ice rather than allowing bubbles to freeze in place above seeps, thereby altering the picture of seep ebullition. All of the seep identification in this study was conducted on ice thicknesses ranging from 10-30 cm, representing approximately 10-40 d of ice growth. Field experiments of blowing bubbles through a tube beneath the ice revealed that with 10-30 cm of ice thickness, bubbles did not substantially migrate away from their seep source.

Variability in CH_4 bubble concentration among lakes may be related to differences in sediment density and gas diffusion rates, depth of the water column through which bubbles travel, sediment organic matter content, nutrient cycling, CH_4 oxidation processes, and groundwater hydrochemistry. Chanton et al. (1989) and Walter et al. (2008a) observed a direct relationship between ebullition and CH_4 concentrations in bubbles due to N_2 stripping from sediments in high-flux ebullition sites. Bubble size and the distance that bubbles travel through the water column is also known to influence bubble concentration at the water surface (Varadharajan 2009; Greinert and McGinnis 2009). The processes that control variability in bubble CH_4 concentrations among arctic and subarctic lakes are not yet well understood. When applying the seep-survey method introduced here, investigators are encouraged to sample gas and determine CH_4 concentrations for ebullition seeps in individual study lakes to ensure they are consistent with seep concentrations we presented here (Table 2).

Application of the method in Siberian and Alaskan lakes revealed large differences in the relative importance of seep ebullition to total-lake CH_4 emissions among lakes. Seep ebullition dominated emissions from Tube Dispenser L. and Shuchi L. (86% to 87% of flux, Fig. 6), but was a smaller component (30%) of emissions from Grass L., a lake in which there was no apparent thermokarst activity an in which partial water column turnover events in September and October led to episodic releases of large quantities of dissolved CH_4 (Fig. 6). The remarkable similarity in CH_4 emissions from Shuchi L. and Tube Dispenser L. (<0.01% relative error), despite their different sizes (47,975 m^2 and 92,238 m^2, respectively, based on June 2008 ALOS PRISM 2.5 m resolution imagery) and independent measurements of diffusion, background bubbling, and ebullition seep distributions, suggests that scaling up measurements for lakes of a similar type to larger regional scales would not result in as much of an error term as scaling up emissions based on lakes that are differ substantially in ebullition within a region, such as those near Toolik Field Station (Fig. 8).

The largest source of variability in applying the method was differences in ebullition-seep distributions within in different lake zones. Variability among transects on individual lakes near Toolik Lake Field Station and Grass Lake in Siberia (24%-173% relative error) was less than variability among zones of the active thermokarst lakes in Siberia, Shuchi and Tube Dispenser (222%-234% relative error), suggesting that thermokarst is a particularly important process fueling CH_4 production in lakes (Zimov et al. 1997; Walter et al. 2006). Ecological, cryogenic, and hydrological processes that govern the distribution and availability of organic matter in lake bottoms are the most likely explanation for differences in seep ebullition among zones in northern lakes, and such processes should be considered in experimental designs employing the ice-bubble survey method.

Comments and recommendations

Until now CH_4 fluxes from northern lakes and wetlands have been underestimated because of a lack of methods for assessing the patchiness of discrete seep bubbling from lakes. Introduction of this simple new technique—mapping CH_4 bubble clusters in lake ice to quantify discrete ebullition-seep emissions— has great potential to improve scientists' ability to estimate lake CH_4 emissions. Lake-ice surveys of ebullition seeps should be integrated with other methods such as floating chambers, headspace equilibration, eddy covariance, and

remote sensing to more accurately assess the magnitude and seasonality of CH_4 emission from individual lakes.

We recommend several areas of research for further improvement upon this method. Logic suggests that there should be a relationship between seep ebullition and the size of ice-bubble clusters. Possible explanations for why we did not observe this relationship include the separation of bubbles by wobble during ascent through the water column and sediment texture. We found that bubble density within clusters was independent of water column depth. Regarding sediment texture, densely packed sediments may channel bubbles more tightly at the sediment-water interface than loose sediments. We suggest that bubble cluster size should be recorded in ice bubble surveys in the event that relationships accounting for bubble density are elucidated in future methods improvement.

Another process that has not been adequately studied in relationship to lake-CH_4 budgets is the potential influence of CH_4 oxidation on ebullition emissions. The mean CH_4 concentrations of fresh seep bubbles released from lake sediments was estimated at 73% to 78% CH_4 in this study. However, this does not necessarily reflect the concentrations of CH_4 released to the atmosphere after gas has been trapped by winter lake ice. Walter et al. (2008a) found isotopic enrichment and a ~30% reduction in CH_4 concentration in ice bubbles, which they attributed to CH_4 oxidation. It is conceivable that bubbles trapped beneath the ice, in contact with relatively O_2-rich lake water before becoming encapsulated in ice, are subject to aerobic CH_4 oxidation. While the apparent oxidation of CH_4, assumed by the enrichment of $\delta^{13}C_{CH4}$ and simultaneous depletion of $\delta^{13}C_{CO2}$ in bubbles observed in this study, was an artifact of sampling (trapping bubbles in submerged traps); this finding raises important questions about the magnitude, seasonality, biogeochemical pathways (aerobic versus anaerobic), and governing factors of CH_4 oxidation in northern lakes that could have a large impact on net annual CH_4 emissions.

Finally, the seasonality of lake CH_4 emissions requires further investigation. During the ice-free season, CH_4 was released directly to the atmosphere by diffusion, background bubbling, and seep ebullition. During the ice cover season, we assumed that diffusion was negligible, and we observed that background ebullition was close to zero. Isotopic analysis and radiocarbon dating of background ebullition bubbles suggested that these bubbles originate in surface sediments of lakes (Walter et al. 2008a), where cold temperatures in winter cause methanogenesis to slow down or cease. Seep ebullition, however, continued throughout winter, and is assumed to be associated with a lag in heat propagation to deeper sediments in winter where CH_4 production fueling ebullition seeps occurs year round (Walter et al. 2008a; Vas et al. 2010). Combined, dissolved CH_4 stored in lake water beneath ice (Michmerhuizen et al. 1996; Phelps et al. 1998) and a large portion of seep CH_4 accumulated in lake ice throughout winter, are subject to large seasonal pulse release in spring when ice melt leads to the disintegration of gas pockets. Application of eddy covariance techniques above lakes would be useful to improve quantification of the seasonality of CH_4 emissions from lakes.

Authorship

K.M. Walter Anthony conceived the experiment, performed the field and laboratory research, and wrote the paper. D Vas developed the automated bubble trap design, measured long-term seep ebullition on the interior Alaska lake, and contributed to the seep class designations. L Brosius contributed to the stable isotope and CH_4 concentration determinations and to interpretation of seep class designations. S.A. Zimov and F.S. Chapin III contributed substantially to the experimental design and writing, respectively. Q. Zhuang performed the biogeochemical modeling experiment. All authors commented on the data analysis, presentation, and writing.

References

Baker-Blocker, A., T. M. Donahue, and K. H. Mancy. 1977. Methane flux from wetland areas. Tellus 29:245-250 [doi:10.1111/j.2153-3490.1977.tb00731.x].

Barber, L. E., and J. C. Ensign. 1979. Methane formation and release in a small Wisconsin lake. Geomicrobiol. J. 1:341-353 [doi:10.1080/01490457909377740].

Bartlett, K. B., P. M. Crill, D. I. Sebacher, R. C. Harriss, J. O. Wilson, and J. M. Melack. 1988. Methane flux from the Central Amazonian Floodplain. J. Geophys. Res. 93:1571-1582 [doi:10.1029/JD093iD02p01571].

———, ———, R. L. Sass, R. C. Harriss, and N. B. Dise. 1992. Methane emissions from tundra environments in the Yukon-Kuskokwim Delta, Alaska. J. Geophys. Res. Atm. 97:16645-16660.

Bastviken, D., J. Cole, M. Pace, and L. Tranvik. 2004. Methane emissions from lakes: Dependence of lake characteristics, two regional assessments, and a global estimate, Global Biogeochem. Cycles 18 [doi:10.1029/2004GB002238].

Boucher, O., P. Friedlingstein, B. Collins, and K. P. Shine. 2009. The indirect global warming potential and global temperature change potential due to methane oxidation. Environ. Res. Letters 4:1-6 [doi:10.1088/1748-9326/4/4/044007].

Casper, P., S. C. Maberly, G. H. Hall, and B. J. Finlay. 2000. Fluxes of methane and carbon dioxide from a small productive lake to the atmosphere. Biogeochem. 49:1-19 [doi:10.1023/A:1006269900174].

Chanton, J. P. 2005. The effect of gas transport mechanism on the isotope signature of methane in wetlands. Organic Geochem. 36:753-768 [doi:10.1016/j.orggeochem.2004.10.007].

———, C. S. Martens, and C. A. Kelley. 1989. Gas transport from methane-saturated, tidal freshwater and wetland sediments. Limnol. Oceanogr. 34:807-819 [doi:10.4319/lo.1989.34.5.0807].

Chen, Y.-H., and R. G. Prinn. 2006. Estimation of atmospheric methane emission between 1996 and 2001 using a three-dimensional global chemical transport model. J. Geophys.

Res. 111 [doi:10.1029/2005JD006058].

Cicerone, R. J., and R. S. Oremland. 1988. Biogeochemical aspects of atmospheric methane. Global Biogeochem. Cyc. 2(4):299-327 [doi:10.1029/GB002i004p00299].

Fallon, R. D., S. Harris, R. S. Hanson, and T. D. Brock. 1980. The role of methane in internal carbon cycling in Lake Mendota during summer stratification. Limnol. Oceanogr. 25:357-360 [doi:10.4319/lo.1980.25.2.0357].

Glaser, P. H., and others. 2004. Surface deformations as indicators of deep ebullition fluxes in a large northern peatland. Glob. Biogeochem. Cyc. 18 [doi:10.1029/2003gb002069].

Grant, R. F., and N. R. Roulet. 2002. Methane efflux from boreal wetlands: Theory and testing of the ecosystem model Ecosys with chamber and tower flux measurements. Glob. Biogeochem. Cyc. 16, 1054. [doi:10.1029/2001GB001702].

Greinert, J., and D. F. McGinnis. 2009. Single bubble dissolution model: the graphical user interface SiBu-GUI. Environ. Mod. Software [doi:10.1016/j.envsoft.2008.12.011].

Grosse, G., K. Walter, and V. E. Romanovsky. 2008. Assessing the spatial and temporal dynamics of thermokarst, methane emissions, and related carbon cycling in Siberia and Alaska, NASA #NNX08AJ37G. April 2008-March 2011 <http://www.gi.alaska.edu/snowice/Permafrost-lab/projects/projects_active/proj_thermokarst_NASA.html>.

Hamilton, J. D., C. A. Kelly, J. W. M. Rudd, R. H. Hesslein, and N. T. Roulet. 1994. Flux to the atmosphere of CH_4 and CO_2 from wetland ponds on the Hudson Bay Lowlands (HBLs). J. Geophys. Res. Atmos. 99:1495-1510.

Huttunen, J. T., and others. 2003. Fluxes of methane, carbon dioxide and nitrous oxide in boreal lakes and potential anthropogenic effects on the aquatic greenhouse gas emissions. Chemosphere 52:609-621 [doi:10.1016/S0045-6535(03)00243-1].

Intergovernmental Panel on Climate Change (IPCC). 2007. Fourth assessment report, the physical science basis, Cambridge Univ. Press.

Joyce, J., and P. W. Jewell. 2003. Physical controls on methane ebullition from reservoirs and lakes. Environ. Engin. Geosci. 9(2):167-178 [doi:10.2113/9.2.167].

Juutinen, S., J. Alm, T. Larmola, J. T. Huttunen, M. Morero, P. J. Martikainen, and J. Silvola. 2003. Major implication of the littoral zone for methane release from boreal lakes. Glob. Biogeochem. Cyc. 17 [doi:10.1029/2003gb002105].

———, and others. 2009. Methane dynamics in different boreal lake types. Biogeoscience 6:209-223 [doi:10.5194/bg-6-209-2009].

Keller, M., and R. F. Stallard. 1994. Methane emission by bubbling from Gatun Lake, Panama. J. Geophys. Res. 99:8307-8319 [doi:10.1029/92JD02170].

Kling, G. W., G. W. Kipphut, and M. C. Miller. 1992. The flux of CO_2 and CH_4 from lakes and rivers in arctic Alaska. Hydrobiologia 240:23-36.

Matthews, E. 2000. Wetlands, pp. 202-233. *In*: M.A.K. Khalil (ed.), Atmospheric methane: its role in the global environment. Springer Verlag.

———, and I. Fung. 1987. Methane emission from natural wetlands: Global distribution, area, and environmental characteristics of sources. Global Biogeochem. Cyc. 1(1):61-86.

Mattson, M. D., and G. E. Likens. 1990. Air pressure and methane fluxes. Nature 347:718-719.

Michmerhuizen, C. M., R. G. Striegl, and M. E. McDonald. 1996. Potential methane emission from north-temperate lakes following ice melt. Limnol. Oceanogr. 41:985-991 [doi:10.4319/lo.1996.41.5.0985].

Miller, L. G., and R. S. Oremland. 1988. Methane efflux from the pelagic regions of four lakes. Glob. Biogeochem. Cyc. 2:269-277 [doi:10.1029/GB002i003p00269].

Mostakhov, S. E. 1973. Ozernost' crioolitozony SSSR, pp. 118-120. *In*: N.I. Tolstikhin (ed.), Mezhdunardonaya conferentsia po merzlotovedeniiu, vol. 5. Podzemnye vody kriolitosfery, Iakutskoe Knizhnoe Izdatel'stvo, Iakkutsk.

Naiman, R. J., T. Manning, and C. A. Johnston. 1991. Beaver population fluctuations and tropospheric methane emissions in boreal wetlands. Biogeochemistry 12:1-15 [doi:10.1007/BF00002623].

Nakayama, T., Y. Nojiri, and Y. Zeng. 1994. Measurement of methane flux from alasses around Yakutsk, eastern Siberia in 1993, pp. 40-44. *In*: G. Inoue. [ed.], Proceedings of the Second Symposium on the Joint Siberian Permafrost Studies between Russia and Japan in 1993. Natl. Inst. for Environ. Studies.

Phelps, A. R., K. M. Peterson, and M. O. Jeffries. 1998. Methane efflux from high-latitude lakes during spring ice melt. J. Geophys. Res. Atmos. 103:29029-29036 [doi:10.1029/98JD00044].

Riera, J. L., J. E. Schindler, and T. Kratz. 1999. Seasonal dynamics of carbon dioxide and methane in two clear-water and two bog lakes in northern Wisconsin, U.S.A. Can. J. Fish. Aquat. Sci. 56:265-274 [doi:10.1139/cjfas-56-2-265].

Riordan, B., D. Verbyla, and A. D. McGuire. 2006. Shrinking ponds in subarctic Alaska based on 1950-2002 remotely sensed images. J. Geophys. Res. 11 [doi:10.1029/2005JG000150].

Roulet, N. T., and others. 1994. Role of Hudson Bay lowland as a source of atmospheric methane. J. Geophys. Res. 99:1439-1454 [doi:10.1029/93JD00261].

———, P. M. Crill, N. T. Comer, A. Dove, and R. A. Boubonniere. 1997. CO_2 and CH_4 flux between a boreal beaver pond and the atmosphere. J. Geophys. Res. 102:29313-29319 [doi:10.1029/97JD01237].

Rudd, J. W. M., and R. D. Hamilton. 1978. Methane cycling in a eutrophic shield lake and its effects on whole lake metabolism. Limnol. Oceanogr. 23:337-348 [doi:10.4319/lo.1978.23.2.0337].

———, R. Harris, C. A. Kelly, and R. E. Hecky. 1993. Are hydro-

electric reservoirs significant sources of greenhouse gases? Ambio 22:246-248.

Semiletov, I. P. 1999. Aquatic sources and sinks of CO_2 and CH_4 in the polar regions. J. Atmos. Sci. 56:286-306 [doi:10.1175/1520-0469(1999)056<0286:ASASOC>2.0.CO;2].

Smith, L. K., and W. M. Lewis Jr. 1992. Seasonality of methane emissions from five lakes and associated wetlands of the Colorado Rockies. Glob. Biogeochem. Cyc. 6:323-338 [doi:10.1029/92GB02016].

Strayer, R. F., and J. M. Tiedje. 1978. In situ methane production in a small, hypereutrophic, hard-water lake: Loss of methane from sediments by vertical diffusion and ebullition. Limnol. Oceanogr. 23:1201-1206 [doi:10.4319/lo.1978.23.6.1201].

Striegl, R. G., and C. M. Michmerhuizen. 1998. Hydrologic influence on methane and carbon dioxide dynamics at two north-central Minnesota lakes. Limnol. Oceanogr. 43:1519-1529 [doi:10.4319/lo.1998.43.7.1519].

Tokida, T., T. Miyazaki, M. Mizoguchi, O. Nagata, F. Takakai, A. Kagemoto, and R. Hatano. 2007. Falling atmospheric pressure as a trigger for methane ebullition from peatland. Global Biogeochem. Cyc. 12 [doi:1029/2006GB2002790].

U.S. Cold Regions Research & Engineering Laboratory (CRREL). 1999. Safety on floating ice sheets, Hanover, New Hampshire, USACE Engineer Research and Development Center. <http://www.crrel.usace.army.mil/ierd/ice_safety/safety.html>

Varadharajan, C. 2009. Magnitude and spatio-temporal variability of methane emissions from a eutrophic freshwater lake, Ph.D. thesis. Massachusetts Institute of Technology

Vas, D.A., K. M. Walter Anthony, R. Barry, P. Anthony. 2010. Understanding the plumbing of methane ebullition seeps in interior Alaska thermokarst-lake sediments from high temporal resolution seep monitoring. MSc. Project Report, Water and Environmental Research Center, University of Alaska, Fairbanks, 90pp.

Walter, B. P., M. Heimann, and E. Matthews. 2001. Modeling modern methane emissions from natural wetlands. 1. Model description and results. J. Geophys. Res. Atmos. 106:34189-34206 [doi:10.1029/2001JD900165].

Walter, K. M., S. A. Zimov, J. P. Chanton, D. Verbyla, and F. S. Chapin III. 2006. Methane bubbling from Siberian thaw lakes as a positive feedback to climate warming. Nature 443:71-75 [doi:10.1038/nature05040].

Walter, K. M., L. C. Smith, and F. S. Chapin III. 2007. Methane bubbling from northern lakes: present and future contributions to the global methane budget. Phil. Trans. Royal Soc. A 365(1856):1657-1676 [doi:10.1098/rsta.2007.2036].

———, J. P. Chanton, F. S. Chapin III, E. A. G. Schuur, and S. A. Zimov. 2008a. Methane production and bubble emissions from arctic lakes: Isotopic implications for source pathways and ages. J. Geophys. Res. 113 [doi:10.1029/2007JG000569].

———, M. Engram, C. Duguay, M. Jeffries, and F. S. Chapin III. 2008b. Potential use of synthetic aperture radar (SAR) for estimating methane ebullition from arctic lakes. J. Amer. Water Res. Assoc. 44(2):305-315.

Whalen, S. C., and W. S. Reeburgh. 1990. A methane flux transect along the trans-Alaska pipeline haul road. Tellus 22B:237-249.

Zhuang, Q., and others. 2004. Methane fluxes between terrestrial ecosystems and the atmosphere at northern high latitudes during the past century: A retrospective analysis with a process-based biogeochemistry model. Glob. Biogeochem. Cyc. 18:1-23 [doi:10.1029/2004GB002239].

Zimov, S. A., and others. 1997. North Siberian lakes: A methane source- fueled by Pleistocene Carbon. Science 277:800-802 [doi:10.1126/science.277.5327.800].

———, Y. V. Voropaev, S. P. Davidov, G. M. Zimova, A. I. Davydova, F. S. Chapin III, and M. C. Chapin. 2001. Flux of methane from North Siberian aquatic systems: Influence on atmospheric methane, pp. 511-524. *In*: R. Paepe and V. Melnikov [eds.], Permafrost response on economic development, environmental security and natural resources. Kluwer.

Submitted 3 January 2010
Revised 22 August 2010
Accepted 14 September 2010